Aalborg Universitet

Thermal analysis of multi-MW two-level wind power converter

Zhou, Dao; Blaabjerg, Frede; Mogens, Lau; Tonnes, Michael

IEEE

Thermal analysis of multi-MW two-level wind power converter

Dao Zhou
Frede Blaabjerg
Lau Mogens
Michael Tonnes

Suggested Citation

Thermal Analysis of Multi-MW Two-level Wind Power Converter

Dao Zhou, Frede Blaabjerg

Department of Energy Technology
Aalborg University
Pontoppidanstraede 101, Aalborg, DK-9220, Denmark
zda@et.aau.dk, fbl@et.aau.dk

Mogens Lau, Michael Tonnes

Danfoss Silicon Power GmbH

Husumer Strasse 251, Flensburg, D-24941, Germany
mogens.lau@danfoss.com, michael.tonnes@danfoss.com

Abstract- **In this paper, the multi-MW wind turbine of partial-scale and full-scale two-level power converter with DFIG and direct-drive PMSG are designed and compared in terms of their thermal performance. Simulations of different configurations regarding loss distribution and junction temperature in the power device in the whole range of wind speed are presented and analyzed. It is concluded that in both partial-scale and full-scale power converter the most thermal stressed power device in the generator-side converter will have higher mean junction temperature and larger junction temperature fluctuation compared to grid-side converter at the rated wind speed. Moreover, the thermal performance of the generator-side converter in the partial-scale power converter becomes crucial around the synchronous operating point and should be considered carefully.**

I. INTRODUCTION

Over the last two decades, the wind power industry has expanded greatly, and has become the fastest developing renewable energy technology in this period. In response to the steady growth of wind power demand, lower cost per kWh, increased power density and higher reliability of wind turbines are essential parameters [1]-[3]. Power electronic converters, as efficient interface between power grid and wind generator, play a key role in wind power generation system. Although the power level of single wind turbine is even pushed up to 7 MW, the size power ratings of 1.5-3 MW are still the dominating on the commercial market. Furthermore, wind turbine converters are being designed for a lifetime of 20-25 years, which is more prolonged compared to typical industrial applications. Therefore the thermal behavior of the power devices is an important factor affecting lifetime of the converter.

Some researchers have already focused on the evaluation of the thermal profile. The thermal stress with partial-scale converter is investigated and it points out an unbalanced thermal performance among different legs at around the particular synchronous operating point [4]. In [5], several promising multilevel configurations with full-scale power converter are compared regarding the thermal behavior of the power devices. As stated in [6], the cycle numbers to failure is

quite relevant to the junction temperature fluctuation as well as the mean junction temperature of power semiconductor.

The scope of this paper is to compare and analyze the thermal profile of multi-MW wind turbine with low-voltage partial-scale and full-scale power converter. First, the typical configurations for variable speed wind turbine system will be briefly introduced. Then, the basic design and the control strategy will be described. Finally loss distribution and thermal analysis will be presented and compared in respect to the power device performance for the two different configurations.

II. TYPICAL CONFIGURATIONS

Due to the extensive and well-established knowledge, as well as the simpler structure and fewer components, the two-level back-to-back voltage source converter is the most attractive solution in commercial market of wind turbines [3]. The utilization of the power electronics in wind turbine system can be further divided into two categories, namely: a wind turbine system with partial-scale power converter and a wind turbine system with full-scale power converter, which both are illustrated in Fig. 1.

A. Wind turbine system with partial-scale power converter
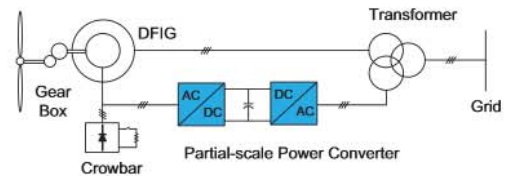
(a) Wind turbine system with partial-scale power converter
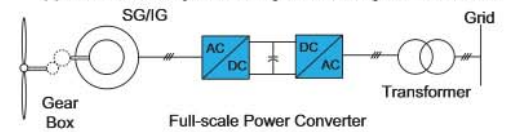
(b) Wind turbine system with full-scale power converter
Fig. 1. Typical configurations for wind turbine system.

A popular wind turbine configuration, normally based on Doubly-Fed Induction Generator (DFIG), is to employ a

power converter rated to approximate by 30% of the nominal generator power and it is shown in Fig. 1a.

The power converter is connected to the rotor through the slip-rings and makes the rotor current as well as rotor speed under control, while the stator links to the grid without any decoupling. If the generator operates in super-synchronous mode, the electrical power is delivered through both the rotor and stator. If the generator is running sub-synchronously, the electrical power is only delivered into the grid from the stator.

The fraction of slip power through the converter makes this concept attractive from an economical point of view. However, the main drawbacks lie in the use of slip rings, and also an additional crowbar is needed to protect the generator-side converter under grid faults [7].

B. Wind turbine system with full-scale power converter

As shown in Fig. 1b, another full-scale power converter configuration equipped with Synchronous Generator (SG) or Induction Generator (IG) is considered as a promising technology for multi-MW wind turbine system.

The generator stator winding is connected to the grid through the full-scale power converter, which performs the reactive power compensation and a smooth grid connection for the entire speed. Some variable speed wind turbine system may become gearless by introducing the multi-pole generator.

The elimination of the slip rings, simpler gearbox and full power controllability during the grid faults are the main advantages. However, in order to satisfy the power rating, the widely used approach nowadays is to implement several converter modules or power devices in parallel, which of course are challenging the complexity and reliability of the whole wind turbine system.

III. BASIC DESIGN OF POWER CONVERTER

As the partial-scale power converter is normally realized by DFIG, while the full-scale power converter matches a direct-drive Permanent Magnet Synchronous Generator (PMSG), for simplicity, these two configurations are called the DFIG system and the PMSG system respectively. In order to evaluate and compare the thermal performance for the above two systems, the mathematical model and simulation platform will firstly be established.

A. Wind turbine model

A 2 MW wind turbine system is used for the case studies. The energy transferred from the kinetic wind power to mechanical power can be expressed as [8]

$$P_G = \frac{1}{2} \rho \pi R^2 C_p(\lambda, \beta) v_w^3 \tag{1}$$

where ρ denotes the air density (kg/m^3), R denotes the radius of turbine blade (m), and v_w denotes the wind speed (m/s). Depending on the blade pitch angle β and tip speed ratio λ, the power coefficient C_p represents the transfer efficiency, whose maximum value can be obtained under optimal tip speed ratio. As claimed in [9], the parameters of the wind turbine are summarized in Table I. Meanwhile, the relationship between

the wind speed and turbine rotor speed, produced output power is depicted in Fig. 2.

TABLE I
PARAMETERS FOR 2 MW WIND TURBINE (DFIG/PMSG)

Wind turbine parameters	
Rated power P_G [MW]	2
Blade radius R [m]	41.3
Cut-in wind speed v_{wcut_in} [m/s]	4
Rated wind speed v_{w_rate} [m/s]	12
Cut-off wind speed v_{wcut_off} [m/s]	25
Optimal tip speed ratio λ_{opt}	8.1
Maximum power coefficient C_{pmax}	0.383
Rated turbine speed n_{rot_rate} [rpm]	19
Minimum turbine speed n_{rot_min} [m/s]	11/6
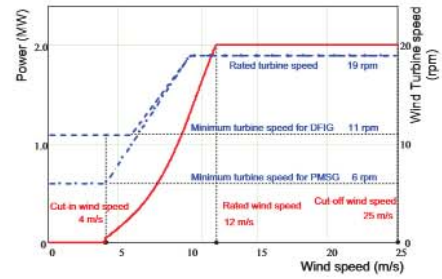
Fig. 2. Relationship between wind speed, turbine rotor speed and output power for the two different systems.

B. Control scheme for DFIG system
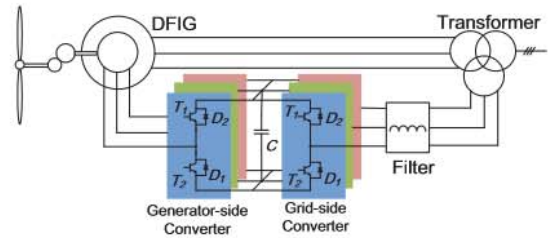
Fig. 3. Two-level back-to-back converter of the DFIG system.

Fig. 3 shows a DFIG system that consists of a generator, a partial-scale power converter, a filter and a transformer. Since the stator is directly connected to low-voltage grid, the DC-link voltage is set as low as possible from the power device lifetime point of view. Moreover, the filter inductance is designed to limit the current ripple within 0.25 pu [10].

Due to the DC capacitor decoupling, the power converter can be divided into the generator-side converter and the grid-side converter. Each of the control schemes can be designed separately.

For the generator-side converter, although the generator may operate in super-synchronous or sub-synchronous mode,

one of the control objectives focuses on transferring the produced active power to the grid. The other purpose is to provide the excited current for the DFIG. As shown in Fig. 4 ("Generator-side control"), the active and reactive power in the stator can be described by rotor d-axis and q-axis current respectively when applied to the stator voltage oriented control [11]. Furthermore, since the coupling current in d-axis and q-axis is induced by Park-transformation, feed-forward compensation method is used to offset their influence. Therefore, the reference of d-axis current is determined by the produced active power, while the reference of q-axis is related to desired reactive power in the stator of the DFIG.

The grid-side converter will keep the DC-link voltage fixed and meet the reactive power demand according to the grid codes. As shown in Fig. 4 ("Grid-side control"), the active and reactive power can simply be controlled by d-axis and q-axis current using the grid voltage oriented control. This control strategy contains two cascaded loops. The inner loop takes care of the grid current; the outer loops control the DC-link voltage and reactive power for the grid-side converter. The DC-link voltage is closely dependent on the active power, thus the adjustment can be regarded as the reference of the d-axis current. Normally, a unity power factor is required, in other words, the reference of q-axis is set to zero unless the grid operator needs reactive power compensation. Furthermore, Space-vector Pulse Width Modulation (SVPWM) is used to generate the switching signals for the power semiconductors in both converters.
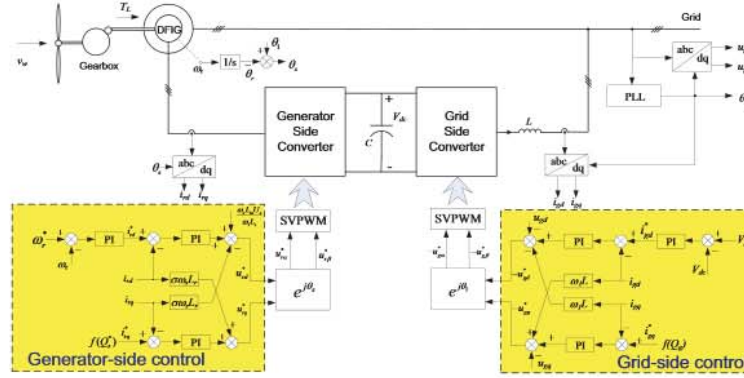

Fig. 4. Control scheme for the DFIG system with Generator-side and Grid-side control.

C. Control scheme for PMSG system

The typical PMSG system equipped with a full-scale power converter is shown in Fig. 5, which consists of a generator-side converter and a grid-side converter. Compared to the DFIG system, the current through both converters will be much higher under same power rating of the wind turbines, which means the selection of power devices in the two configurations will be quite different in order to realize similar power device loading. Nevertheless, the design method of the DC-link voltage and the filter inductance in the PMSG system can be referred to the DFIG system.
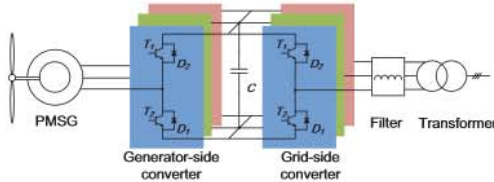

Fig. 5. Two-level back-to-back converter in a PMSG system.

Considering the control scheme of the generator-side converter, the current through the stator of the generator should be controlled to adjust the rotating speed for maximum power. As shown in Fig. 6 ("Generator-side control"), this can easily be achieved by controlling the electromagnetic torque through a closed loop control structure with the aid of the stator Field Oriented Control (FOC), where the electromagnetic torque is controlled indirectly through the stator current in the synchronous reference frame. The torque is only controlled by q-axis current component. The cascaded loop structure of the generator-side converter is realized by three PI-controllers: one speed controller and two current controllers. The outer PI-controller controls the mechanical speed of the generator and produces the q-axis current reference for inner current controller. On the contrary, the reference of the d-axis current is set to zero for minimum power loss [8]. Compensation terms are added to improve the dynamic response.

For the grid–side converter, the outer DC-link voltage and inner current closed loop have the ability to perform a fast active power performance and to control the injected or absorbed reactive power, which are almost the same as the grid-side converter in a DFIG system.

IV.   POWER LOSS MODELLING

In order to compare the different two-level back-to-back wind power converter configurations, analysis of the loss distribution will be presented in this section.

A. Power device selection

As mentioned, the produced energy through the power converter semiconductors is quite different in the DFIG and

the PMSG system. Consequently, it is important to select the suitable power devices for both systems in order to obtain a fair comparison for the thermal loading.
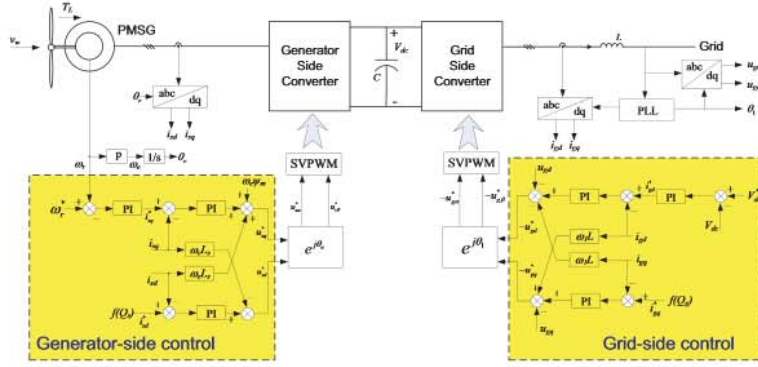

Fig. 6. Control scheme for the PMSG system with Generator-side and Grid-side control.

It is assumed that the two systems are using the wind turbine system as illustrated in Table I. Typical parameters for the generators are summarized in Table II. The PMSG system is a direct-drive for multi-pole structure, while for the DFIG system, a gearbox is still required as a multi-pole low-speed DFIG is not technically feasible.

TABLE II

2 MW GENERATOR DATA FOR DFIG AND PMSG [11], [12]

	DFIG	PMSG
Rated wind speed v_{w_rate} [m/s]	12	
Rated turbine speed n_{rot_rate} [rpm]	19	
Number of pole pairs p	2	102
Gear ratio	94.7	/
Rated shaft speed n_s [rpm]	1800	19
Rated fundamental frequency f_e [Hz]	10	32.3
Stator leakage inductance L_{ls} [mH]	0.038	0.276
Magnetizing inductance L_m [mH]	2.91	
Rotor leakage inductance L_{lr} [mH]	0.064	/
Stator/rotor turns ratio n	0.369	/

The most important data for the two-level back-to-back converter are listed in Table III. The switching frequency in both configurations and both converters are set to 2 kHz. The rated active power in the DFIG system is much smaller than the PMSG system, as only slip power flows through both converters. Based on the active power, together with the rated converter voltage output, the current in the converter needs to be calculated.

It is noted that in the DFIG system the rated current in the grid-side converter and the generator-side converter is much more unequal, while the situation is better in the PMSG system. Furthermore, a parallel structure of multiple power components is a more used solution for multi-MW wind turbines today. Consequently, a common 1700V/1000A power device is selected. A single module in the grid-side converter and two paralleled modules in the generator-side converter are

the solutions for the DFIG system, and four paralleled modules in both converters for the PMSG system are selected.

TABLE III

TWO-LEVEL BACK-TO-BACK POWER CONVERTER DATA

	DFIG	PMSG
Rated active power P_C [kW]	400	2000
DC-link voltage U_{dc} [Vdc]	1050	
Switching frequency f_s [kHz]	2	
Grid-side Converter		
Rated output voltage [Vrms]	704	704
Rated current [Arms]	328	1641
Filter inductance [mH]	0.50	0.15
Generator-side Converter		
Rated output voltage [Vrms]	374	554
Rated current [Arms]	618	2085

B. Power loss calculation

The power losses in the back-to-back converter consist of the generator-side converter loss and the grid-side converter loss. They are mainly divided into the switching losses and the conduction losses. Since no unbalance is taken into account in this paper, it is possible to consider the behavior of half of one leg in both side converters due to the symmetrical characteristic and the fixed DC-link voltage.

No matter what the current direction is, the switching losses in each switching period always contain one turn-on loss E_{on}, one turn-off loss E_{off} in the IGBT, and one diode recovery loss E_{rr}. E_{on}, E_{off} and E_{rr} are almost proportional to the DC-link voltage, thus the formula for switching loss in each power device P_{sw} can be expressed as:

$$P_{sw} = f_e \frac{U_{dc}}{U_{dc}^*} \sum_{n=1}^{N} \left[E_{on}(|i_a(n)|) + E_{off}(|i_a(n)|) + E_{rr}(|i_a(n)|) \right] \quad (2)$$

where f_e denotes the fundamental frequency of the phase current, U_{dc}^* denotes the tested DC-link voltage, N denotes the

total cycle numbers in each fundamental frequency, E_{on}, E_{off} and E_{rr} denote the switching loss energy in each switching period when the switching current equals to the phase current $|i_a(n)|$. E_{on}, E_{off}, E_{rr} and U_{dc}^* can be directly acquired from the power device datasheets.

The conduction losses mainly lie in the IGBT and the freewheeling diode. The conduction power loss in each power device P_{con} can be calculated as:

$$P_{con} = f_e \sum_{n=1}^{N} \left[v_{CE}(|i_a(n)|) \cdot |i_a(n)| \cdot T_1(n) + v_F(|i_a(n)|) \cdot |i_a(n)| \cdot (T_s - T_1(n)) \right] \quad (3)$$

where v_{CE} denotes the collector-emitter saturation voltage drop of the IGBT, v_F denotes the forward on-state voltage drop of the freewheeling diode, $T_1(n)$ denotes the conduction time of the IGBT during n^{th} switching period, which in line with the modulation strategies and the phase angle between phase current and phase voltage. T_s denotes the switching period.

C. Power loss distribution in the systems

Simulation of the power loss can be realized based on PLECS block in Simulink [13]. The simulation settings correspond to the design parameters shown in Table II and Table III. In addition, the simulation circuit runs at rated wind speed under normal grid condition and the power factor is set to unity. Fig. 7 and Fig. 8 indicate the loss distribution of each power semiconductor under the DFIG and the PMSG systems in terms of the generator-side converter and the grid-side converter, respectively. The name of the power semiconductor can be found in Fig. 3 and Fig. 5.

TABLE IV

PARAMETERS FOR CONVERTERS AT DIFFERENT WIND SPEED (DFIG/PMSG)

Wind speed [m/s]	Generator power [MW]	Wind turbine speed [rpm]	Slip	Fundamental frequency [Hz]
5.9	0.26	11/10.1	0.3/0	15/17.2
6.8	0.39	12.7/12.0	0.2/0	10/20.4
7.6	0.55	14.2/13.7	0.1/0	5/23.3
8.4	0.74	15.8/15.4	0/0	0/26.2
9.2	0.98	17.2/17.1	-0.1/0	5/29.1
10.1	1.29	19/19	-0.2/0	10/32.3
12	2	19/19	-0.2/0	10/32.3
25	2	19/19	-0.2/0	10/32.3

Comparing the back-to-back power converter in both systems, the power losses dissipated in the generator-side converter are more equal. It is because the turn-on and turn-off loss of IGBT are higher than the recovery loss of freewheeling diode for the same current, from (2) the switching loss in the diode is always smaller. The conduction loss is mainly related to the power direction. At rated active power, the generator-side converter is operating as a rectifier, and therefore more conduction losses are seen in the freewheeling diode. On the contrary, the grid-side converter is operating as an inverter, where most conduction losses are dissipated in the IGBT, which result in an unequal loading.

For the DFIG and the PMSG systems, the power loss dissipated in the PMSG system is larger. The reason is that as

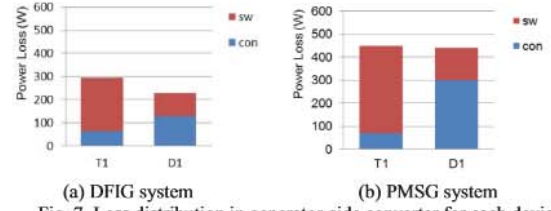summarized in Table III, the current through each power semiconductor is higher.

(a) DFIG system   (b) PMSG system
Fig. 7. Loss distribution in generator-side converter for each device (wind speed: 12 m/s).

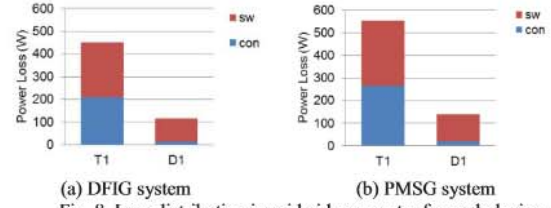

(a) DFIG system   (b) PMSG system
Fig. 8. Loss distribution in grid-side converter for each device (wind speed: 12 m/s).
Note: **sw** and **con** are switching losses and conduction losses, respectively

In order to investigate the loss behavior in different operation modes, several wind speeds are chosen with slip values from -0.3 to 0.2 in the DFIG system and shown in Table IV. It is noted that the wind speed at 8.4 m/s is regarded as the synchronous operating point as it is seen in Fig. 2 and in Table II.
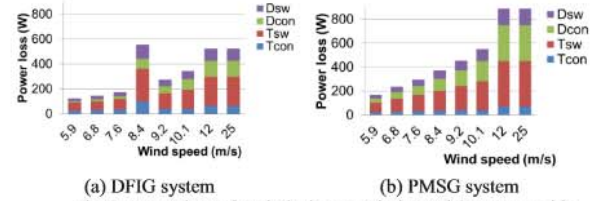

(a) DFIG system   (b) PMSG system
Fig. 9. Power loss of each device vs. wind speed (generator-side converter).
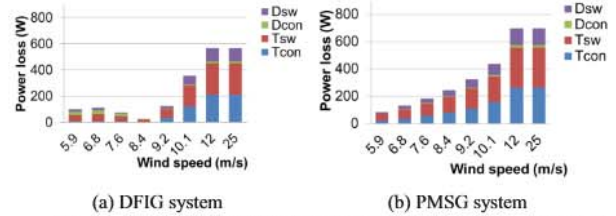

(a) DFIG system   (b) PMSG system
Fig. 10. Power loss of each device vs. wind speed (grid-side converter).

The power loss in the generator-side converter at different wind speed is shown in Fig. 9. At synchronous operating point of the DFIG system, the rotor current becomes the DC component, the power loss in three legs will be significantly unbalanced. The most stressed IGBT and diode are illustrated in Fig. 9a, whose power loss is even higher than those at rated wind speed. In the super-synchronous mode, the power loss increases with larger wind speed, and the growth rate is relatively slower since the larger slip, which will decrease the converter current. It is noted that the conduction loss in the diode is dominating. However, in the sub-synchronous mode,

the conduction loss in the IGBT is dominating. For the PMSG system, the power loss increases with the wind speed consecutively.

The power loss in the grid-side converter at different wind speed is shown in Fig. 10. For the DFIG system, the lowest power loss appears in the synchronous operating point due to the fact that no active power flow and only the switch ripple current affects, while the highest one appears at rated wind power. Furthermore, the IGBT suffers more loss in super-synchronous mode and the diode suffers more loss in sub-synchronous mode. For the PMSG system, the power loss increases with the wind speed consecutively.

V. THERMAL ANALYSIS OF THE SYSTEMS

As the thermal performance of the power devices are closely related to the reliability and the cost of the whole power converter system, a comparison of the thermal cycling of the DFIG and the PMSG systems are done.

A. Thermal model

In order to describe the thermal behavior of the power semiconductors, an appropriate thermal model needs to be developed. The thermal models of single IGBT and the freewheeling diode are shown in Fig. 11, and share the same design idea as discussed in [5], the thermal resistance R_{th} will determine the steady-state mean junction temperature, and along with the thermal capacitance (function of time constant τ) will determine the junction temperature fluctuation.
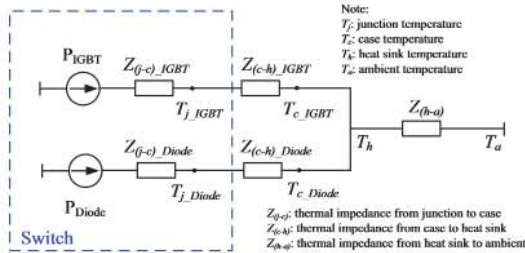

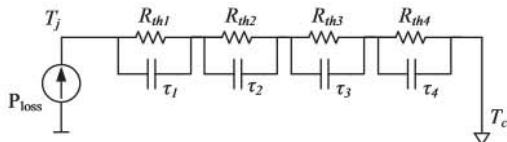Fig. 11. Thermal models of the power semiconductors.

Fig. 12. RC Foster network of thermal impedance from junction to case of the power semiconductor devices.

The thermal impedance from the junction to case $Z_{(j-c)}$ is modeled as four-layer Foster RC network as depicted in Fig. 12, whose parameters are collected from the datasheet of the power device. The case-to-heatsink thermal impedance is modelled as a simple thermal resistor, neglecting the much higher thermal capacitance due to the less significant dynamic behavior of junction temperature and faster thermal simulation. Meanwhile the heatsink-to-ambient resistance is considered small compared to the thermal resistance in the

MW power converter. Furthermore, the ambient temperature is set to 50 °C.

B. Analysis of thermal cycling

The simulation results of the junction temperature in each power semiconductor of the generator-side converter under the DFIG and the PMSG systems are shown in Fig. 13 in which the converters run at rated power and in steady-state operation. It can be seen that the mean temperature of the diode is higher than the IGBT's in both the DFIG and the PMSG systems, and the thermal performance of the PMSG system shows more unequal distribution, where the difference of junction temperature between the IGBT and the diode is 12.4 °C compared to 5.1 °C in the DFIG system. For the junction temperature of the grid-side converter, the thermal results of the DFIG and the PMSG systems are shown in Fig. 14a and Fig. 14b respectively. It can be seen that the hottest power semiconductor device turns out to be the IGBT. Moreover, the junction temperature variation between the IGBT and the diode show more equal distribution.
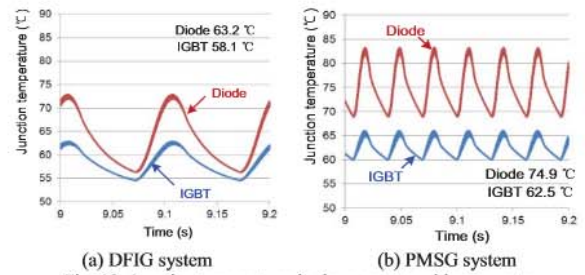

(a) DFIG system   (b) PMSG system
Fig. 13. Junction temperature in the generator-side converter (Wind speed: 12 m/s).

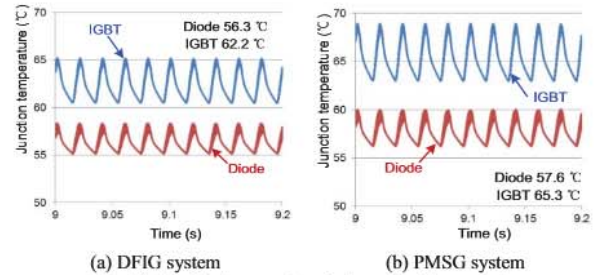(a) DFIG system   (b) PMSG system
Fig. 14. Junction temperature in the grid-side converter (Wind speed: 12 m/s).

A further comparison of thermal behavior for both systems with different wind speed is shown in Fig. 15. For the generator-side converter, it can be seen that, in the PMSG system the mean junction temperature and the temperature fluctuation of the power semiconductors above rated wind speed are the highest among the whole operation range of the wind. The hottest device is the diode in the whole range of the wind speed. In the DFIG system, the hottest device changes from the IGBT in the sub-synchronous mode to the diode in the super-synchronous mode. Moreover, the mean junction temperature and the temperature fluctuation of the power semiconductors become crucial around the synchronous operating point. Although the mean junction temperature is all

higher in the PMSG system except for the region around synchronous operation as shown in upper Fig. 15a, at rated wind speed the temperature fluctuation in the DFIG system is even larger due to less frequency power loss cycling as shown in lower Fig. 15a. For the grid-side converter in the PMSG system, the mean junction temperature and the junction temperature fluctuation of power semiconductors above rated wind speed becomes the highest in the whole operation range of the wind. In the DFIG system, the hottest device changes from the diode in the sub-synchronous mode to the IGBT in the super-synchronous mode. Moreover, the mean junction temperature as well as the junction temperature fluctuation becomes the least crucial around the synchronous operating point. As the power loss of the PMSG system is higher than the DFIG system, the mean junction temperature is higher in the PMSG system as shown in upper Fig. 15b. Moreover, the junction temperature fluctuation in the DFIG system is smaller due to same frequency power loss cycling as shown in lower Fig. 15b under rated wind speed.
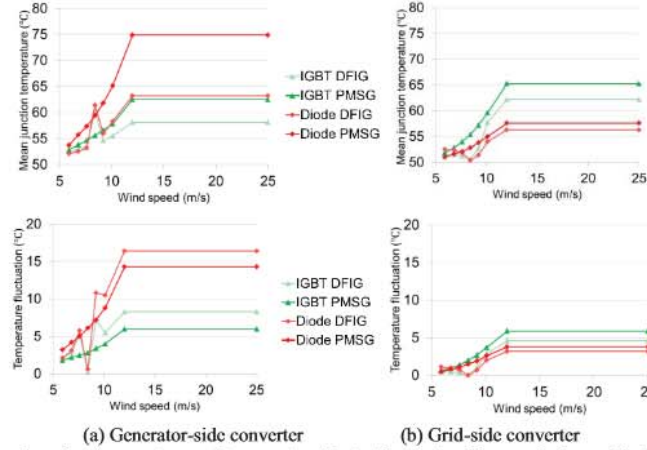

(a) Generator-side converter   (b) Grid-side converter

Fig. 15. Mean junction temperature and temperature fluctuation in the chip vs. wind speed for both systems.

VI. CONCLUSION

In this paper, platforms for the popular 2 MW two-level wind turbine configurations (i.e. partial-scale and full-scale power converter) are established in the PLECS/Simulink to simulate the power losses and the thermal load cycling. A comparison of the loss distribution as well as thermal loading in the DFIG and the PMSG systems are investigated.

For the partial-scale power converter configuration, the thermal behavior between the generator-side converter and the grid-side converter are quite different. The operation area above the rated wind speed range of the grid-side converter is significant from the thermal stress point of view, while the generator-side converter not only concerns the above mentioned case, but also the wind speed range around the synchronous operation.

For the full-scale power converter configuration, whatever generator-side converter or grid-side converter, the crucial thermal stress lies in the operation area above the rated wind speed range.

Moreover, comparing the most stressed semiconductor device, the generator-side converter is the most critical part for thermal stress of the two-level back-to-back converter for high power applications. Furthermore, the reactive power support to the grid as well as the wind speed variation will affect the thermal profile of the power semiconductors.

References

[1] Z. Chen, J.M. Guerrero, F. Blaabjerg, "A review of the state of the art of power electronics for wind turbines," *IEEE Trans. on Power Electronics*, vol.24, no.8, pp.1859-1875, Aug. 2009.

[2] F. Blaabjerg, Z. Chen, S.B. Kjaer, "Power electronics as efficient interface in dispersed power generation systems," *IEEE Trans. on Power Electronics*, vol.19, no.5, pp. 1184- 1194, Sep. 2004.

[3] M. Liserre, R. Cárdenas, M. Molinas, J. Rodriguez, "Overview of multi-MW wind turbines and wind parks," *IEEE Trans. on Industrial Electronics*, vol.58, no.4, pp.1081-1095, Apr. 2011.

[4] M. Bruns, B. Rabelo, W. Hofmann, "Investigation of doubly-fed induction generator drives behaviour at synchronous operating point in wind turbines," *in Proc. of EPE 09*, pp.1-10, Sep. 2009.

[5] K. Ma, F. Blaabjerg, "Multilevel converters for 10 MW wind turbines," in *Proc. of EPE 11*, pp.1-10, 2011.

[6] A. Wintrich, U. Nicolai, T. Reimamm, "Semikron Application Manual," pp.128, 2011.

[7] F. Blaabjerg, M. Liserre, K. Ma, "Power electronics converters for wind turbine systems," *IEEE Trans. on Industry Applications*, vol.48, no.2, pp.708-719, Mar. 2012.

[8] M. Chinchilla, S. Arnaltes, J.C. Burgos, "Control of permanent-magnet generators applied to variable-speed wind-energy systems connected to the grid," *IEEE Trans. on Energy Conversion*, vol.21, no.1, pp. 130-135, Mar. 2006.

[9] "Vestas." [Online]. Available: http://www.vestas.com/.

[10] A.A. Rockhill, M. Liserre, R. Teodorescu, P. Rodriguez, "Grid-filter design for a multi-megawatt medium-voltage voltage-source inverter," *IEEE Trans. on Industrial Electronics*, vol.58, no.4, pp.1205-1217, Apr. 2011.

[11] C. Liu, F. Blaabjerg, W. Chen, D. Xu, "Stator current harmonic control with resonant controller for doubly fed induction generator," *IEEE Trans. on Power Electronics*, vol.27, no.7, pp.3207-3220, Jul. 2012.

[12] H. Li, Z. Chen, H. Polinder, "Optimization of multibrid permanent-magnet wind generator systems," *IEEE Trans. on Energy Conversion*, vol.24, no.1, pp.82-92, Mar. 2009.

[13] User manual of PLECS blockset version 3.2.7 March 2011. (Available: http://www.plexim.com/files/plecsmanual.pdf